

A numerical solution to a model of the BEC-BCS transition

Jonathan Newnham*
(Dated: 2010-03-31)

I. INTRODUCTION

The discovery of high-temperature superconductivity in 1986 [1] resulted in a flurry of theoretical work that continues to this day. The mechanism of high-temperature superconductivity is not fully understood. A full understanding would make development of new superconducting materials economically feasible, with many technological applications in science and industry.

In CUPRATE superconductors it is believed that the superconducting property has something to do with two-dimensional copper-oxide planes. Bardeen-Cooper-Schrieffer (BCS) theory [2] explains low-temperature superconductivity extremely well. The recent discovery of other high-critical-temperature systems [3, 4] involving two-dimensional structures has provided a larger experimental basis against which to test theory.

It is currently infeasible to directly observe electrons moving around in a superconducting solid. In recent years there has been much interest in studying a system with many similarities to BCS systems, that of ultracold gases of fermionic atoms [5–10]. Such gases are superfluids, in the same way that superconducting electrons form a superfluid. In this report, we apply BCS theory to a one-dimensional cloud of fermions in a harmonic trap, and look for evidence of a phase transition, with no fermionic pairing on one side ($\Delta = 0$) and some on the other.

II. THEORY

In this discussion we follow [10, 11]. Unlike Jensen et al, we analyse the one-dimensional case and include the Hartree term in our numerical solution procedure. We also do not assume symmetry around the origin.

We begin with a one-dimensional version of the BCS hamiltonian [2]

$$H = \sum_{\sigma} \int dx \hat{\Psi}_{\sigma}^{\dagger}(x) \left(-\frac{\hbar^2}{2m_{\sigma}} \nabla^2 - \mu_{\sigma} + V(x) \right) \hat{\Psi}_{\sigma}(x) + \iint dx dx' \hat{\Psi}_{\uparrow}^{\dagger}(x) \hat{\Psi}_{\downarrow}^{\dagger}(x') U(x-x') \hat{\Psi}_{\downarrow}(x') \hat{\Psi}_{\uparrow}(x) \quad (1)$$

where $V(x) = 1/2m\omega^2x^2$ is a harmonic potential. This is sensible as any trap is harmonic to first order and so this matches with the experimental traps used in other studies [8, 9] quite well. Here, $\hat{\Psi}_{\sigma}(x)$ and $\hat{\Psi}_{\sigma}^{\dagger}(x)$ are the real space annihilation and creation operators of a particle with spin σ at position x . We approximate the interaction as $U(x-x') = \delta(x-x')U$, which is reasonable as the actual Coulomb interaction goes as x^{-6} .

We now apply the mean-field approximation. The first step is to define

$$\Delta(x) \equiv U \left\langle \hat{\Psi}_{\uparrow}(x) \hat{\Psi}_{\downarrow}(x) \right\rangle$$

$$\Delta^*(x) \equiv U \left\langle \hat{\Psi}_{\downarrow}^{\dagger}(x) \hat{\Psi}_{\uparrow}^{\dagger}(x) \right\rangle$$

which is the mean overlap between opposite spins as a function of x . We now have

$$U \hat{\Psi}_{\uparrow}^{\dagger} \hat{\Psi}_{\downarrow}^{\dagger} \hat{\Psi}_{\downarrow} \hat{\Psi}_{\uparrow} = U \left(\frac{1}{U} \Delta^* + \frac{1}{U} \delta^{\dagger}(x) \right) \left(\frac{1}{U} \Delta + \frac{1}{U} \delta(x) \right) \quad (2)$$

where

$$\frac{1}{U} \delta^{\dagger}(x) \equiv \hat{\Psi}_{\uparrow}^{\dagger}(x) \hat{\Psi}_{\downarrow}^{\dagger}(x) - \frac{1}{U} \Delta^*(x)$$

describes the deviations about the mean. The mean-field approximation takes these deviations to be small, such that $\delta^{\dagger}\delta$ is negligible. Expanding (4) and discarding the $\delta^{\dagger}\delta$ term, we find

$$U \hat{\Psi}_{\uparrow}^{\dagger} \hat{\Psi}_{\downarrow}^{\dagger} \hat{\Psi}_{\downarrow} \hat{\Psi}_{\uparrow} = -\frac{1}{U} \Delta^* \Delta + \Delta^* \hat{\Psi}_{\downarrow} \hat{\Psi}_{\uparrow} + \Delta \hat{\Psi}_{\uparrow}^{\dagger} \hat{\Psi}_{\downarrow}^{\dagger}.$$

The $\Delta^*\Delta$ term is the mean field of the interaction (not an operator) and hence provides a constant offset to the eigenenergies. It is thus not interesting when considering interactions between particles, so we absorb it into the constant part of the hamiltonian H_0 .

The second part of the mean-field approximation is to define

$$n_{\sigma}(x) \equiv \left\langle \hat{\Psi}_{\sigma}^{\dagger}(x) \hat{\Psi}_{\sigma}(x) \right\rangle. \quad (3)$$

This allows an alternative expansion of

$$U \hat{\Psi}_{\uparrow}^{\dagger} \hat{\Psi}_{\downarrow}^{\dagger} \hat{\Psi}_{\downarrow} \hat{\Psi}_{\uparrow} = U \hat{\Psi}_{\uparrow}^{\dagger} \hat{\Psi}_{\uparrow} \hat{\Psi}_{\downarrow}^{\dagger} \hat{\Psi}_{\downarrow} = U (n_{\uparrow} + \delta_{\uparrow}(x)) (n_{\downarrow} + \delta_{\downarrow}(x)) \quad (4)$$

where

$$\delta_{\sigma}(x) \equiv \hat{\Psi}_{\sigma}^{\dagger}(x) \hat{\Psi}_{\sigma}(x) - n_{\sigma}(x).$$

We once again assume that the fluctuations around the mean number of particles are small and expand (4) to get

$$U \hat{\Psi}_{\uparrow}^{\dagger} \hat{\Psi}_{\downarrow}^{\dagger} \hat{\Psi}_{\downarrow} \hat{\Psi}_{\uparrow} = -U n_{\uparrow} n_{\downarrow} + U n_{\uparrow} \hat{\Psi}_{\downarrow}^{\dagger} \hat{\Psi}_{\downarrow} + U n_{\downarrow} \hat{\Psi}_{\uparrow}^{\dagger} \hat{\Psi}_{\uparrow}$$

Performing both of these expansions is necessary because they take into account different types of fluctuations.

Putting all this together, we arrive at the mean-field Hamiltonian

$$H_{MF} = \sum_{\sigma} \int dx \hat{\Psi}_{\sigma}^{\dagger}(x) \left(-\frac{\hbar^2}{2m_{\sigma}} \nabla^2 - \mu_{\sigma} + V(x) \right) \hat{\Psi}_{\sigma}(x) + \sum_{\sigma} \int dx U n_{\sigma}(x) \hat{\Psi}_{-\sigma}^{\dagger}(x) \hat{\Psi}_{-\sigma}(x) + \int dx \left(\Delta(x) \hat{\Psi}_{\uparrow}^{\dagger}(x) \hat{\Psi}_{\downarrow}^{\dagger}(x) + H.c. \right)$$

*Electronic address: jnnewn@pgrad.unimelb.edu.au

In order to diagonalise H_{MF} we expand $\hat{\Psi}$ in terms of the eigenstates of a harmonic trap:

$$\hat{\Psi}_\sigma(x) \equiv \sum_n R_n(x) \hat{a}_{n\sigma} \quad (5)$$

where

$$R_n(x) \equiv (2^n n! \sqrt{\pi})^{-1/2} H_n(x) e^{-x/2}$$

with H_n the Hermite polynomials. Inserting these definitions yields

$$\begin{aligned} H_{MF} = & \sum_{n,\sigma} (\varepsilon_n - \mu_\sigma) \hat{a}_{n\sigma}^\dagger \hat{a}_{n\sigma} + U \sum_{n,n',\sigma} J_{nn'\bar{\sigma}} \hat{a}_{n\sigma}^\dagger \hat{a}_{n'\sigma} \\ & + \sum_{n,n'} F_{nn'} \hat{a}_{n\uparrow}^\dagger \hat{a}_{n'\downarrow} + H.c. \end{aligned} \quad (6)$$

where the H_0 eigenstate energies $\varepsilon_n = \hbar\omega(n + 1/2)$. The number interaction, in which a large number n_σ in one polarization changes the chemical potential of the other polarization $\mu_{\bar{\sigma}}$, is described by the elements

$$J_{nn'\sigma} = \int_{-\infty}^{\infty} dx R_n(x) n_\sigma(x) R_{n'}(x).$$

The pairing field, in which it may be energetically favourable to create pairs of highly-entangled particles instead of single ones, is described by

$$F_{nn'} = \int_{-\infty}^{\infty} dx R_n(x) \Delta(x) R_{n'}(x).$$

In this basis, the density of spin σ atoms is obtained by combining (3) and (5) to give

$$n_\sigma(x) = \sum_{n,n'} R_n(x) R_{n'}(x) \langle \hat{a}_{n\sigma}^\dagger \hat{a}_{n'\sigma} \rangle \quad (7)$$

and similarly

$$\Delta(x) = U \sum_{n,n'} R_n(x) R_{n'}(x) \langle \hat{a}_{n\uparrow}^\dagger \hat{a}_{n'\downarrow} \rangle. \quad (8)$$

In order for this problem to be computationally feasible, we now introduce a limit to sums over n , N_c . This is allowable because the states we are ignoring in this process are high-energy and thus have very low occupation levels, and so ignoring them should have a negligible effect on the solution (as long as N_c is high enough to incorporate all states with a reasonable degree of occupancy). This limitation allows us to write (6) matrix form:

$$H_{MF} = \begin{pmatrix} \hat{a}_{0\uparrow}^\dagger \\ \vdots \\ \hat{a}_{N_c\uparrow}^\dagger \\ \hat{a}_{0\downarrow} \\ \vdots \\ \hat{a}_{N_c\downarrow} \end{pmatrix}^T M \begin{pmatrix} \hat{a}_{0\uparrow} \\ \vdots \\ \hat{a}_{N_c\uparrow} \\ \hat{a}_{0\downarrow} \\ \vdots \\ \hat{a}_{N_c\downarrow} \end{pmatrix} \quad (9)$$

with

$$M = \begin{pmatrix} \varepsilon_0 - \mu_\uparrow + U J_{00\downarrow} & \cdots & U J_{0N_c\downarrow} & F_{00} & \cdots & F_{0N_c} \\ \vdots & \ddots & \vdots & \vdots & \ddots & \vdots \\ U J_{N_c 0\downarrow} & \cdots & \varepsilon_{N_c} - \mu_\uparrow + U J_{N_c N_c\downarrow} & F_{N_c 0} & \cdots & F_{N_c N_c} \\ F_{00}^* & \cdots & F_{0N_c}^* & -\varepsilon_0 + \mu_\downarrow - U J_{00\downarrow} & \cdots & -U J_{N_c 0\uparrow} \\ \vdots & \ddots & \vdots & \vdots & \ddots & \vdots \\ F_{N_c 0}^* & \cdots & F_{N_c N_c}^* & -U J_{0N_c\uparrow} & \cdots & -\varepsilon_{N_c} + \mu_\downarrow - U J_{N_c N_c\uparrow} \end{pmatrix}.$$

We now introduce the basis that diagonalises H_{MF} by the definition of γ_j ,

$$H_{MF} \equiv \sum_{j=0}^{2N_c+1} E_j \hat{\gamma}_j^\dagger \hat{\gamma}_j, \quad (10)$$

where $\hat{\gamma}$ are the eigenstates and E_j the eigenenergies. In this basis, H_{MF} is diagonal. The $\hat{\gamma}$ basis is related to the harmonic oscillator basis by the Bogoliubov transforma-

tion (defining the unitary \hat{W}),

$$\begin{pmatrix} \hat{a}_{0\uparrow} \\ \vdots \\ \hat{a}_{N_c\uparrow} \\ \hat{a}_{0\downarrow} \\ \vdots \\ \hat{a}_{N_c\downarrow} \end{pmatrix} \equiv \hat{W} \begin{pmatrix} \hat{\gamma}_{0\uparrow} \\ \vdots \\ \hat{\gamma}_{N_c\uparrow} \\ \hat{\gamma}_{0\downarrow} \\ \vdots \\ \hat{\gamma}_{N_c\downarrow} \end{pmatrix}. \quad (11)$$

Inserting (11) into (9) yields

$$H_{MF} = \begin{pmatrix} \hat{\gamma}_{0\uparrow} \\ \vdots \\ \hat{\gamma}_{N_c\uparrow} \\ \hat{\gamma}_{0\downarrow} \\ \vdots \\ \hat{\gamma}_{N_c\downarrow} \end{pmatrix}^\dagger \hat{W}^\dagger M \hat{W} \begin{pmatrix} \hat{\gamma}_{0\uparrow} \\ \vdots \\ \hat{\gamma}_{N_c\uparrow} \\ \hat{\gamma}_{0\downarrow} \\ \vdots \\ \hat{\gamma}_{N_c\downarrow} \end{pmatrix}$$

and comparing with our definition of $\hat{\gamma}$ (10) demonstrates that $\hat{W}^\dagger M \hat{W}$ must be the diagonal matrix of energy eigenvalues E . We thus find that \hat{W} is the eigenvector matrix of M (or that the columns of \hat{W} are the eigenvectors of M) via the equation

$$M \hat{W} = \hat{W} E = E \hat{W}.$$

In the $\hat{\gamma}$ basis, the density of atoms in the \uparrow state is, from (7) and (11),

$$\begin{aligned} n_\uparrow(x) &= \sum_{n,n'=0}^{N_c} R_n(x) R_{n'}(x) \\ &\times \left\langle \left(\sum_j W_{jn} \hat{\gamma}_j^\dagger \right) \left(\sum_{j'} W_{j'n} \hat{\gamma}_{j'} \right) \right\rangle \quad (12) \\ &= \sum_j \sum_{n,n'=0}^{N_c} R_n(x) R_{n'}(x) W_{jn} W_{j'n} \langle \hat{\gamma}_j^\dagger \hat{\gamma}_j \rangle \\ &= \sum_j \sum_{n,n'=0}^{N_c} R_n(x) R_{n'}(x) W_{jn} W_{j'n} n_F(E_j) \quad (13) \end{aligned}$$

where $n_F(E) = 1 / (1 + e^{E/k_B T})$ is the Fermi distribution as the γ states are orthogonal. This means the γ states do not interact with each other, and occupation levels are

given by the Fermi distribution. Similarly,

$$\begin{aligned} n_\downarrow(x) &= \sum_j \sum_{n,n'=0}^{N_c} R_n(x) R_{n'}(x) \\ &\times W_{j,n+N_c+1} W_{j,n'+N_c+1} n_F(-E_j) \end{aligned}$$

and

$$\begin{aligned} \Delta(x) &= U \sum_j \sum_{n,n'=0}^{2N_c+1} R_n(x) R_{n'}(x) \\ &\times W_{jn} W_{j,n'+N_c+1} (1 + 2n_F(E_j)). \end{aligned}$$

Integrating over x in (13) gives

$$\begin{aligned} N_\uparrow &= \sum_j \sum_{n=0}^{N_c} W_{jn} W_{jn} n_F(E_j) \\ N_\downarrow &= \sum_j \sum_{n=0}^{N_c} W_{j,n+N_c+1} W_{j,n+N_c+1} n_F(-E_j). \end{aligned}$$

We now have all the equations we need. To solve them we will use a self-consistent approach: Start with a guess for W_{jn} and E_j and use that to calculate $n_\uparrow(x)$ and $n_\downarrow(x)$, and hence $F_{nn'}$ and $J_{nn'}$; this will allow us to calculate (along with a guesses for μ_\uparrow and μ_\downarrow) M , from which we can find new (hopefully more accurate) values for W_{jn} and E_j . Performing this procedure repeatedly hopefully converges the matrix to a correct solution. If we want a specific N_\uparrow and N_\downarrow then we can adjust the μ_\uparrow and μ_\downarrow at each iteration, as a larger chemical potential μ normally leads to an increased number of particles N .

There is an important simplification to reduce the complexity of the problem significantly. Calculating $F_{nn'}$ can be done much more efficiently by observing that

$$\begin{aligned} F_{nn'} &= \int_{-\infty}^{\infty} dx R_n(x) \Delta(x) R_{n'}(x) \\ &= \int_{-\infty}^{\infty} dx R_n(x) R_{n'}(x) \sum_{jmm'} R_m(x) R_{m'}(x) + W_{jm} W_{j,m'+N_c+1} (1 + 2n_F(E_j)) \\ &= \sum_j \sum_{m,m'}^{2N_c+1} W_{jm} W_{j,m'+N_c+1} (1 + 2n_F(E_j)) \int_{-\infty}^{\infty} dx R_n R_{n'} R_m R_{m'} \end{aligned}$$

and there exists an efficient way of calculating the integral, namely

$$\begin{aligned} \int_{-\infty}^{\infty} dx R_a(x) R_b(x) R_c(x) R_d(x) &= \frac{2^{-1/2}}{\pi^2 \sqrt{a!b!c!d!}} \sum_{r=0}^b \frac{1}{r!} \frac{b!}{(b-r)!} \frac{a!}{(a-b+r)!} \Gamma\left(\frac{-(a-b)+c+d+1}{2} - r\right) \\ &\times \Gamma\left(\frac{(a-b)+c-d+1}{2} + r\right) \Gamma\left(\frac{(a-b)-c+d+1}{2} + r\right) \quad (14) \end{aligned}$$

for $a + b + c + d$ even. (This integral is 0 for $a + b + c + d$ odd by symmetry of the Hermite polynomials.)

A similar result can be shown for $J_{nn'}$. This has two

benefits: for large values of n in $R_n(x)$, the function os-

cillates too fast for numerical integration to be practical. Secondly, the closed form solution given above is considerably faster than numerical integration, especially if the Lanczos approximation is used to calculate the Γ -functions. In fact, (14) can be calculated exactly using

$$\Gamma\left(n + \frac{1}{2}\right) = \sqrt{\pi} \frac{(2n-1)!!}{2^n} = \sqrt{\pi} \frac{(2n)!}{2^{2n} n!}.$$

III. IMPLEMENTATION

Our algorithm is given in Figure 1. The basic idea of the algorithm is to continuously adjust the two μ values while iterating the self-dependent equation involving W_{jn} . We adjust the μ values to approach the desired values of N_{\uparrow} and N_{\downarrow} using the bisection algorithm.

At each iteration we plot $n_{\uparrow}(x)$, $n_{\downarrow}(x)$ and $\Delta(x)$.

The convergence criteria are quite strict, requiring $N_{\uparrow}, N_{\downarrow}$, μ_{\uparrow} and μ_{\downarrow} to be determined to within 1% (as tested for by their range. As we are trying to constrain two N values using two μ values (in other words, a two-dimensional optimisation problem) with a function that is constantly evolving, we found that we could not rely on separating the two μ values and performing quasi-1D bisection on each value independently. Instead, we opted to gradually increase the range of μ in the appropriate direction if we found that our N range no longer included the target N . Normally the bisection algorithm halves the target range of μ at each step, choosing a half depending on whether the N corresponding to the midpoint of the μ range is above or below the target N .

One problem we encountered in using (14) is that machine precision issues are encountered in dividing very large numbers by other very large numbers. The double-precision floating point format can only store numbers up to about 10^{308} or $\Gamma(171)$, constraining the maximum N_c to about 50. In our implementation, strange problems occurred with larger N_c s, limiting our maximum N_c to

about 30.

IV. RESULTS

Table II gives a summary of the most interesting results. Some associated plots are given in Figure 2.

Run 12 was interesting because the solver did not converge to a stable solution, oscillating between $n_{\uparrow}(x) = n_{\downarrow}(x)$ with $\mu_{\downarrow} \simeq 4$ (“ n stuck equal”) and n s that were too far apart with $\mu_{\downarrow} \in (1, 3)$. This is probably because, with a polarisation of 2:1, we are near the boundary of a phase transition where a larger polarisation prevents a condensate from forming.

The results investigated six regimes, given in Table I. They showed clear evidence of BCS condensation, heavily dependent on opposing-spin interaction strength U . A strong (more than 2:1) polarisation also prevented condensation.

We also investigated the effect of varying polarisation for strong interactions ($U = -3$, $kT = 1$), in a series of 9 simulations with $N_{\uparrow} = 10$ and $N_{\downarrow} \in [1, 9]$. For $N_{\downarrow} < 6$ our $\Delta(x)$ started behaving unphysically (changing sign). A second run with $U = -5$, $kT = 2$ produced better results, with everything above $N_{\downarrow} = 2$ condensing into a BCS state.

V. CONCLUSION

Our model found clear evidence of BCS condensation, in agreement with experimental papers, and a clear phase separation as suggested by [8]. The next step is to apply this model to a periodic potential, to predict the results of an experiment in which laser interference creates such a potential for the fermionic superfluid. A 3-D box model may also allow inference of the interaction strength U in a real experiment.

[1] J. Bednorz and K. Müller, *Zeitschrift für Physik B Condensed Matter* **64**, 189 (1986).
[2] J. Bardeen, L. Cooper, and J. Schrieffer, *Physical Review* **108**, 1175 (1957).
[3] H. Takahashi, K. Igawa, K. Arii, Y. Kamihara, M. Hirano, and H. Hosono, *Nature* **453**, 376 (2008).
[4] S. Jin, H. Mavoori, C. Bower, and R. Van Dover, *Nature* **411**, 563 (2001).
[5] C. Regal, M. Greiner, and D. Jin, *Physical review letters* **92**, 40403 (2004).
[6] G. Partridge, K. Strecker, R. Kamar, M. Jack, and R. Hulet, *Physical review letters* **95**, 20404 (2005).
[7] M. Zwierlein, J. Abo-Shaer, A. Schirotzek, C. Schunck, and W. Ketterle, *Nature* **435**, 1047 (2005).
[8] G. Partridge, W. Li, R. Kamar, Y. Liao, and R. Hulet, *Science* **311**, 503 (2006).
[9] M. Zwierlein, A. Schirotzek, C. Schunck, and W. Ketterle, *Science* **311**, 492 (2006).
[10] L. Jensen, J. Kinnunen, and P. Törmä, *Physical Review A* **76**, 33620 (2007).
[11] Y. Ohashi and A. Griffin, *Physical Review A* **72**, 13601 (2005).

[12] URL <http://www.ph.unimelb.edu.au/~jnnewn/cm-seminar-results/>.

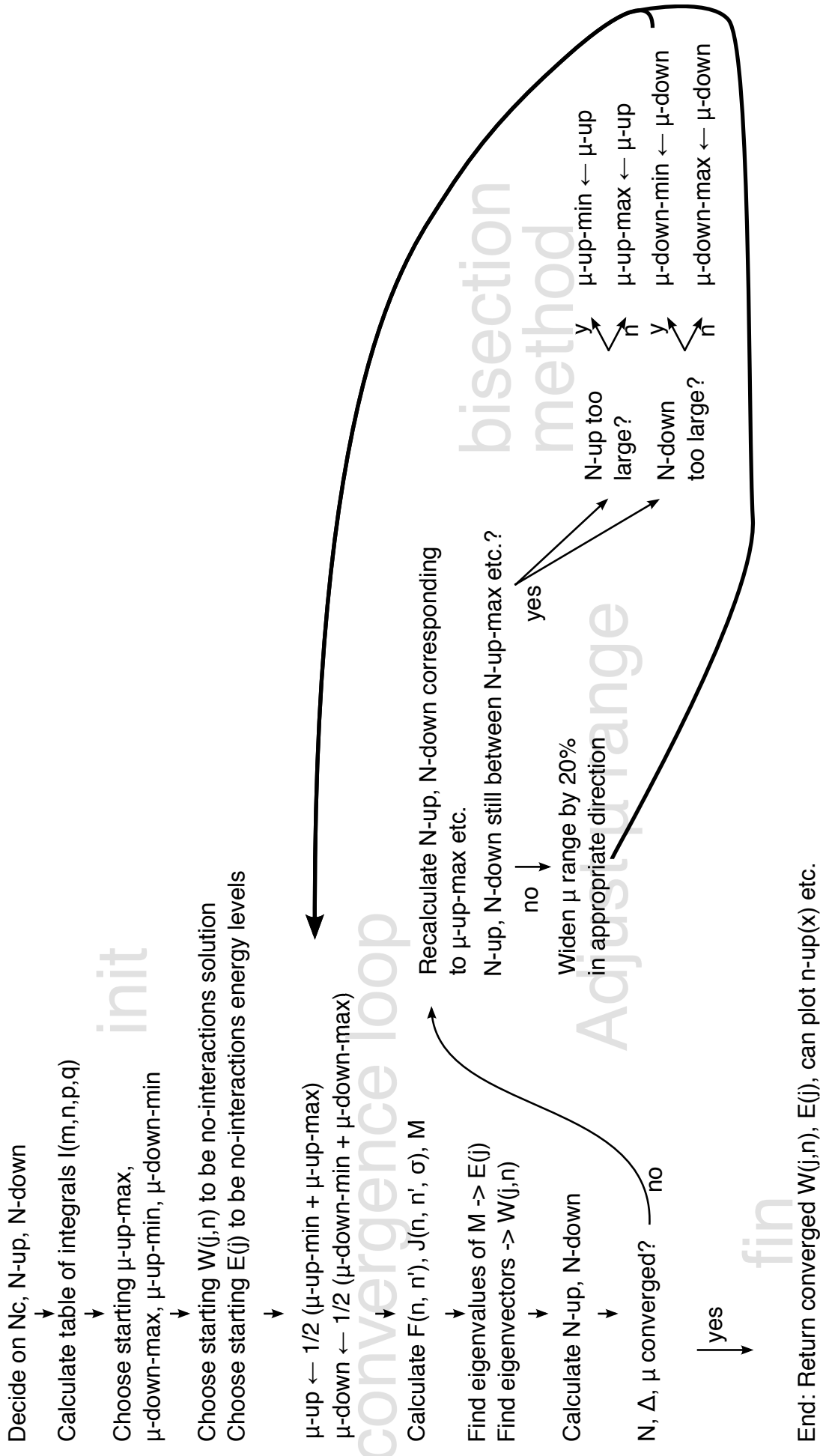


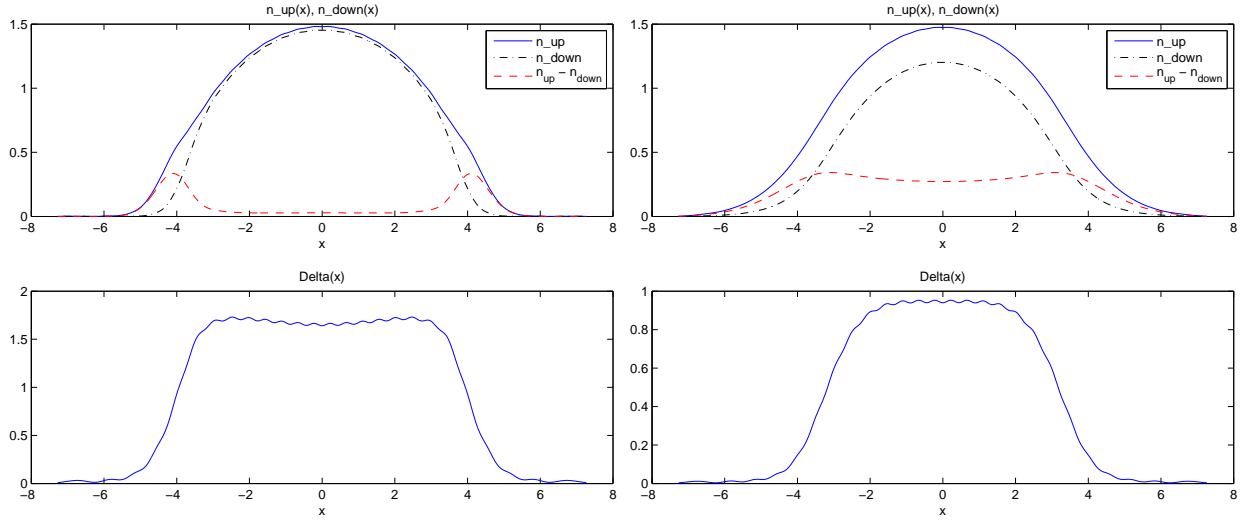
Figure 1: Flow diagram of our implementation.

U	kT	$\hbar\omega$	Condenses?	Sample Runs
Small	Moderate	Large	N	
Small	Large	Moderate	N	19,20
Moderate	Small	Large	N	1,14,16,18,22
Moderate	Large	Small	N	21
Large	Small	Moderate	Y	12,13,15,17
Large	Moderate	Small	Y	2-11

Table I: Investigated Regimes.

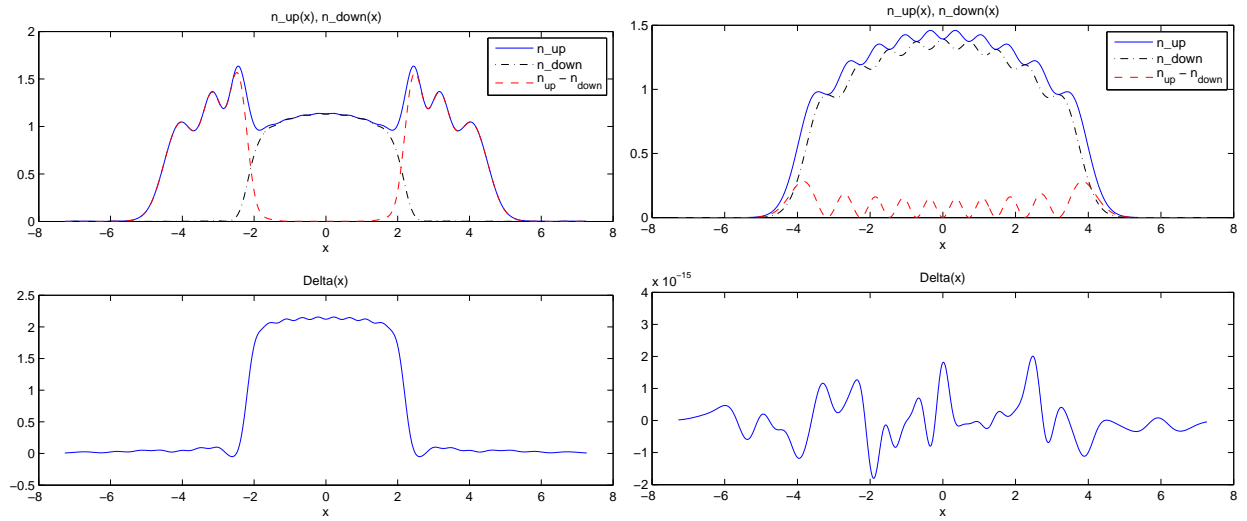
#	N_{\uparrow}	N_{\downarrow}	μ_{\uparrow}	μ_{\downarrow}	U	kT	$\hbar\omega$	Cond?	Comments	Plot
1	10	9	9.2	8.0	-1	1	1	N	All parameters equal... crossover region.	
2	10	9	9	8.8	-3	1	1	Y	Moderate interaction	
3	10	9	7.4	5.9	-3	3	1	N	Moderate interaction, moderate temperature	
4	10	9	10.6	-0.4	-5	1	1	Y	Very strong interactions, halo of excess polarisation	2a
5	10	9	6.5	3.3	-5	3	1	Y	Moderate temperature, strong interaction	
6	10	9	5.5	3.7	-5	4	1	Y	Higher temp., just barely condensed. (Just below T_C)	
7	10	9	5.4	3.5	-5	5	1	N	Higher temp, did not condense – too hot (Just above T_C)	
8	10	7	6.9	0.7	-5	4	1	Y	More polarisation, just barely condensed. (Just below T_C)	2b
9	10	7	8.1	-0.1	-5	3	1	Y	Lower temperature, condensed more easily	
10	10	2	9.0	-6.5	-5	3	1	N	Strong interactions, high polarisation	
11	10	2	9.3	-5.3	-5	1	1	Y	Strange result – $\Delta(x)$ oscillating in sign.	
12	10.5	4.5	11.8	-17.7	-10	10^{-4}	1	Y	Did not converge (μ_{\downarrow} oscillating – “stuck ns ”)	2c
13	9.3	9.3	8.5	5.0	-3	0.01	1	Y	Unconverged (“stuck ns ”)	
14	10	9	9.8	8.9	-0.1	0.01	1	N	Strong confinement, weak interactions	2d
15	10	10	7.4	7.4	-3	0.01	1	Y	Strong interactions, low temperature	
16	10	10	9.7	9.8	-0.1	0.01	1	N	Strong confinement, equal polarisations	
17	10	5	9	1.2	-3	0.01	1	N	Unconverged – $\Delta(x)$ sign oscillating, “stuck ns ”	
18	10	5	10	4.8	-0.1	0.01	1	N	Large polarisation	
19	10	9	8.8	7.3	-0.1	7	1	N	High temperature	
20	10	5	8.8	0.6	-0.1	7	1	N	High temperature, high polarisation	
21	10	9	7.0	5.1	-3	5	1	N	High temperature, moderate interaction	
22	10	9	9.6	8.5	-0.5	0.1	1	N	Strong confinement, moderate interactions	

Table II: Results. Matlab generating code and plots of every run are available at [12].



(a) Run 4. BCS condensation is observed ($\Delta \sim 1$). The unpaired material is expelled from the central region and appears as a halo.

(b) Run 8.



(c) Run 12. An unusual result.

(d) Run 14. An uncondensed state, $\Delta \sim 0$.

Figure 2: Various densities of the two spin states and the associated pairing potential Δ . A large value for Δ indicates that significant condensation into a BCS state has occurred. The ripples in many graphs are due to the small numbers of particles used in our solution – like a Fourier transform of a square wave with a small number of terms, these ripples are a result of the finite sum over Hermite polynomials.